We are very grateful to Daniel Herwartz, assisted by Claudia Voigt, for his in-depth review. As advised, we further worked the modelling part. All the issues raised by the reviewer will be addressed in a revised draft. Answers, point by point, are following:

In their experiment 1, the authors investigate how leaf water composition changes between different growth stages and along the leaf. In the revised version the authors modeled the expected evaporation trend by extending the model of Farquhar and Gan (2003) for 17Oexcess. The model curves are concave in triple oxygen isotope space and clearly differ from the convex model curves recently published for a series of evaporitic ponds (see Surma et al. 2018). Both models are based on the Craig and Gordon model, so this discrepancy comes unexpected. I discussed this puzzling observation with my PhD student Claudia Voigt and she discovered, that calculating the parameter h' both from 17_'s and 18_'s (not just 18_'s) changes the curvature of the model to a convex form (i.e. identical to Surma et al. 2018).

Thanks for pointing out this inaccuracy. We revised the model accordingly:
In Table S4, h is the ratio of ambient humidity to the humidity at the sites of evaporation in the leaf. The parameter h' ($h' = 1-a_{equil} * a_k *(1-h)$) (Farquhar and Gan, 2003) depends on h and the equilibrium and diffusion isotope fractionation values which differ for ^{18}O and ^{17}O (Table S3 of the excel file). As a consequence, h' calculated for ^{18}O ($^{18}h'$ in Table S4) is different from h calculated for ^{17}O ($^{17}h'$ in table S4). Table S4 is corrected accordingly and the revised model curves (Figure 1 below) are convex as the ones presented in Surma et al. (2018) for evaporated lakes.

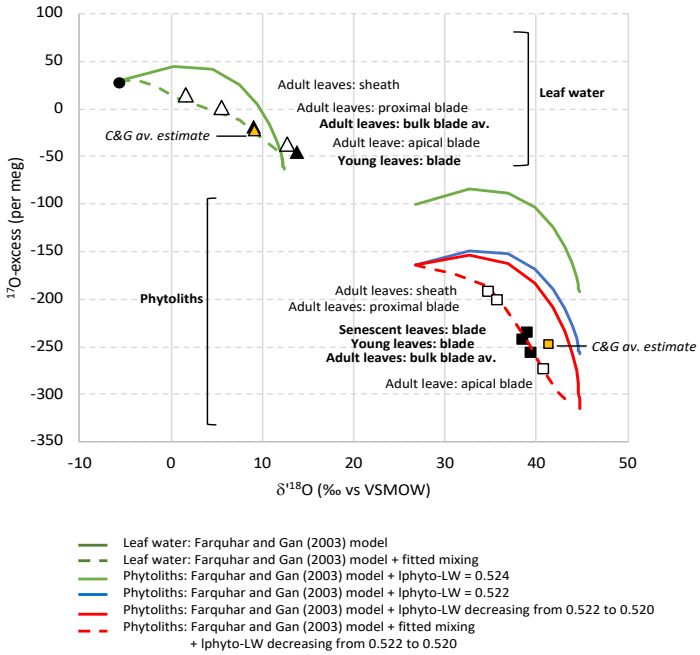

Figure 1. Growth chamber experiment 1: triple oxygen isotope data and model comparisons.

^{17}O-excess vs $\delta'^{18}O$ observed for leaf water (triangles) and phytoliths (squares) in young adult and senescent leaves (black symbols) and along adult leaf (sheath, proximal blade, apical blade) (white symbols) (Table S2).

Predicted curves depicted for leaf water along the leaf according to i) the Farquhar and Gan (2003) model (dark green continuous curve), ii) a mixing between irrigation water and evaporated water estimated from the Farquhar and Gan (2003) model (dark green dashed curve) (Table S4).

Predicted curves depicted for phytoliths along the leaf according to i) the Farquhar and Gan (2003) model and assuming $\lambda_{Phyto-LW} = 0.524$ (Sharp et al., 2016) (light green continuous curve), $\lambda_{Phyto-LW} = 0.522$ (blue continuous curve), $\lambda_{Phyto-LW}$ decreasing from 0.522 to 0.520 from bas to apex (red continuous curve), and ii) a mixing between irrigation water and evaporated water estimated from the Farquhar and Gan (2003) model (red dashed curve) (Table S4).

Craig and Gordon averaged estimates (Cernusak et al., 2016) (Table S3) for leaf water (yellow triangle), and phytoliths (yellow square) assuming $\lambda_{phyto-LW} = 0.521$.

At first sight it appears as if the data fit better to such a revised model but possibly more processes need to be considered (e.g. mixing).

The string-of-lake approach (Farquhar and Gan, 2003) matches well with the $\delta'^{18}O_{LW}$ and $^{17}O\text{-excess}_{LW}$ range of values measured along the leaf. However, between the minimum and maximum values, the $\delta'^{18}O_{LW}$ data are systematically lower than the $\delta'^{18}O_{LW}$ estimates. As advised, for the modelled curve to match the data, a mixing process must be added (Table S3 and S4, Figure 1). In a simplistic way, we hypothesized that part of the initial water (i.e. the irrigation water) entering the grass circulates in the parallel veinal structure of the blade without participating to the pool of water successively evaporated when the length vs maximum length (l/lm in Table S4) increases. The proportion of evaporated water in leaf water and phytolith-forming water (respectively E_{LW} and $E_{phyto\text{-}FW}$ in Table S4) can be fitted from 0 to 1 to match the ^{17}O-excess and $\delta'^{18}O$ evolution with l/lm. The resulting curves are shown in Figure 1 (green dashed curve for leaf water and red dashed curve for phytolith-forming water).

To match the leaf water data, E_{LW} must be close to 0.4, 0.4-0.8, 1 and 0.8-0.9 in the sheath, proximal, apical and averaged adult bulk blade, respectively. To match the phytolith data (assuming a $\lambda_{silica\text{-}water}$ value decreasing from 0. 522 to 0.520), $E_{phyto\text{-}FW}$ must range from 0.6 to 0.7 from the sheath to the apical part of the blade.

The discrepancy between fitted E_{LW} and fitted $E_{phyto\text{-}FW}$ can be explained by the following assumption: phytolith-forming water integrates the whole grass elongation period (Kumar and Elbaum, 2017; Kumar et al., 2016, 2019) while the sampled leaf water only represents a snapshot. As phytoliths form mainly (but not exclusively) in the epidemal cells, $E_{phyto\text{-}FW}$ is higher than E_{LW} in the sheath. Toward the apex, the increase of E_{LW} is balanced by another process: in grass leaf, the epidermal cells are produced at the base of the leaf and are pushed towards the apex through the elongation zone during the growth. Hence leaf epidermal cells that are close to the apex are older than the cells close to the base (Kavanová et al., 2006; Kumar et al., 2019) and phytoliths in these cells gather early and late phytoliths formed at low and high l/lm values with low and high E_{LW} values, respectively.

If the authors manage to improve the plant water model, their paper would become significant for many other fields. Leaf water controls the triple oxygen isotopic composition of O2 (produced from leaf water) and CO2 (equilibrates with leaf water). It's well worth the effort to improve the model.

The Farquhar and Gan (2003) modelling approach, incremented with the $\delta^{17}O$, matches well with the leaf water data experimentally obtained. Along the leaf blade, $\delta'^{18}O_{LW}$ and $^{17}O\text{-excess}_{LW}$ values evolve as a function of the length relatively to the maximum leaf length (l/lm in table S4). This approach implies that whatever is the grass leaf length, the averaged $\delta'^{18}O_{LW}$ and $^{17}O\text{-excess}_{LW}$ values are predictable from the Craig and Gordon model (Cernusak et al., 2016), which is indeed observed. This result is promising for predicting the triple oxygen isotope composition of leaf water per plant functional types or plant traits. This would bring some significant information for i) estimating the triple oxygen isotope composition of CO_2 equilibrated with leaf water and partitioning gross fluxes of CO2 from vegetation (e.g. Helliker and Ehleringer, 2000) or ii) estimating the triple oxygen isotope composition of O_2 produced by the biosphere and quantifying its productivity from air bubbles trapped in ice cores (Blunier et al., 2002), at a global scale.

The above paragraph will be added to the conclusion section of the revised draft.

I found it especially interesting, that the measured phytolith data cannot be modeled from measured leaf water using published equilibrium fractionation factors. If the published equilibrium fractionation factors are correct, kinetic effects must be responsible for the observed offset. Or the measured leaf water is not representative of local leaf water from which the phytoliths form. To me, the changing _ values along the leaf seem to imply that the kinetic effects are not identical over the length of the blade. Is it possible to explain the data via contrasting fractionation factors during active (via enzymes) and/or passive (via evaporation) phytolith formation?

Indeed, the sampled leaf water is likely not the phytolith-forming water, as discussed above. Anyway, the revised model curve obtained for phytoliths (red dashed curve in Figure 1, Farquhar and Gan (2003) model + mixing hypothesis) match with the data only if, $\lambda_{Phyto\text{-}LW}$ decreases regularly from 0.522 to 0.520 from the base to the apex of the blade, i.e. if a kinetic fractionation occurs during silica polymerization, with its amplitude increasing with length. The proportion of long cell phytoliths formed from passive silicification, increases from the base to the apex (Figure 2). This would go against a control of enzymatic processes on the kinetic fractionation. However, on the basis of current knowledge additional experiments are required to further discuss this point.

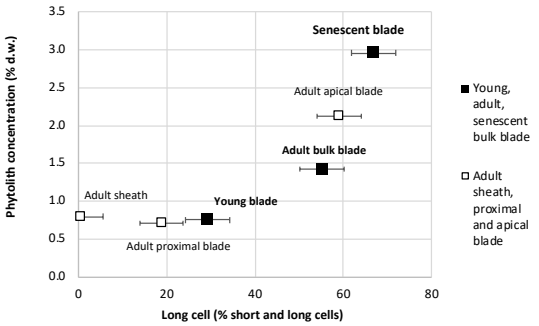

Figure 2. Growth chamber experiment 1 : Phytolith concentration *vs* Long Cell phytolith proportion. Error bars represent the 5% error on counting.

Line 120: The isotopic composition of the vapor in air is identical to that of irrigation water. If these two reservoirs have any chance to exchange, vapor in air would be driven to lower values (i.e. the two reservoirs equilibrate). The agar agar prevents such an exchange to some degree. I assume that water vapor in the air is constantly exchanged to ensure constant RH and vapor isotopic composition. Is this correct? The vapor isotopic composition has a strong effect on the evaporation trajectories in triple oxygen isotope space, so if partial equilibration occurs that would be important to know.

As described in the Material section, ambient relative humidity is kept constant in the growth chamber by combining a flow of dry air and an ultrasonic humidifier that produces vapor without any isotope fractionation. Thus, yes, the water vapor in the air should be constantly exchanged at the growing chamber scale, although, we cannot completely rule out that right above the agar-agar and around the leaves some water vapor comes from the soil water evaporation. Additional (and in progress) experiment including continuous measurement of the atmospheric water vapor will help to further assess this point in a near future.

Line 231: The main reason why the sheath comprises a lower oxygen isotopic composition than the blade is not the lower transpiration rate. As a thought experiment, assume that transpiration rates in the sheath and the blade are identical. The 'source water' of the sheath would be irrigation water with low d18O. But the source water to the blade would be evaporated water from the sheath with somewhat enriched d18O. In this simple model the blade could have a far lower transpiration rate than the sheath and still comprise higher d18O.

Indeed, in this model the isotope composition along the leaf does not depend on transpiration. Thanks for highlighting this inaccuracy which will be corrected in the revised draft. The revised model is now based on the only assumption that the initial water is the irrigation water. The model clearly shows the ^{18}O-enrichment in the sheath water and successive enrichment in the blade (Figure 1).

Model for the prediction of phytoliths in Figure 3: The empirical _Phyto-LW as calculated from this data is used to predict the triple oxygen isotopic composition of the photoliths, which is circular. If the published _silica-water = 0.524 is used, the 17Oexcess values would be far off (as shown in Figure S1). Present the model using _=0.524 in Figure 1 (not only in Figure S1).

Yes, indeed. This is confusing. Figure 1 (above) will be presented in the revised draft (in place of figure 3 and figure S1 in the former draft).

Section 7 (Conclusions): The first paragraph is confusing to me. Grass height and leaf height are mentioned here for the first time. Of course experiment 1 shows that leaf water composition changes along the leaf as predicted by the model, but this fractionation is not related to absolute hight but to l/lm. So a large (or high) leaf would carry the same bulk isotopic information as a short leaf (as stated at the end of paragraph 2). Also, I would not mix up the kinetic effects story with the RH story in the same paragraph.

Thanks for underlying this inaccuracy. For further clarity, in the revised draft the conclusion section will be separated in two paragraphs as follows:

Conclusions

Modelling the triple oxygen iostope composition of grass leaf water

The Farquhar and Gan (2003) modelling approach, incremented with the $\delta^{17}O$, matches well with the leaf water data experimentally obtained. Along the leaf blade, $\delta'^{18}O_{LW}$ and $^{17}O\text{-excess}_{LW}$ values evolve as a function of the length relatively to the maximum leaf length (l/lm in table S4). This approach implies that whatever is the grass leaf length, the averaged $\delta'^{18}O_{LW}$ and $^{17}O\text{-excess}_{LW}$ values are predictable from the Craig and Gordon model (Cernusak et al., 2016), which is indeed observed. This result is promising for predicting the triple oxygen isotope composition of leaf water per plant functional types or plant traits. This would bring some significant information for i) estimating the triple oxygen isotope composition of CO_2 equilibrated with leaf water and partitioning gross fluxes of CO2 from vegetation (e.g. Helliker and Ehleringer, 2000) or ii) estimating the triple oxygen isotope composition of O_2 produced by the biosphere and quantifying its productivity from air bubbles trapped in ice cores (Blunier et al., 2002), at a global scale.

Interpreting the ^{17}O-excess of grass phytolith assemblages

The measured $^{17}O\text{-excess}_{phyto}$ values obtained for adult and senescent leaves are close to the Craig and Gordon averaged $^{17}O\text{-excess}_{LW}$ estimate assuming a fractionation exponent $\lambda_{Phyto\text{-}LW}$ of 0.521. This fractionation exponent, which is lower than the value of 0.524 published for equilibrium $\lambda_{Silica\text{-}water}$ (Sharp et al., 2016), decreases from the base to the apex of the leaf. This result calls for additional data to i) further constrain the equilibrium fractionation exponent $\lambda_{Silica\text{-}water}$, and ii) further assess the occurrence, extent and systematicity of a triple oxygen isotope kinetic fractionation during phytolith formation. The opportunity to predict $^{17}O\text{-excess}_{LW}$ from $^{17}O\text{-excess}_{phyto}$ is worth the effort.

Regarding the measured $\delta'^{18}O_{phyto}$ values obtained for adult and senescent leaves, they are close to the Craig and Gordon averaged $\delta'^{18}O_{LW}$ estimate if a 7/3 mixing of evaporated/unevaporated water is introduced. This bias is likely inherent to the pattern of silica polymerization in the course of the leaf growth. Its extent and variability with grass physiognomy must be tackled.

Anyway, the relevance of using the Farquhar and Gan (2003) modelling approach to explain the $^{17}O\text{-excess}_{phyto}$ evolution with l/lm, added to the agreement of the $^{17}O\text{-excess}_{phyto}$ measured for adult and senescent leaves with the Craig and Gordon averaged $^{17}O\text{-excess}_{LW}$ estimate, support that the $^{17}O\text{-excess}_{phyto}$ dependency on RH should not be biased by the grass length. This is in line with the $^{17}O\text{-excess}_{Phyto}$ values obtained for the adult bulk blade and senescent leaf blade phytoliths (-257 and -235 per meg, respectively) being close to the values estimated from the RH-dependency of $^{17}O\text{-excess}_{Phyto}$ equation obtained in Alexandre et al. (2018) from growth chamber samples (-222 per meg) and natural transect samples (-212 per meg).

In addition to grass leaf length, the stem *vs* leaf biomass ratio can be very heterogeneous from a grass development stage to another and from a grass genus to another. Previous studies showed that phytoliths from grass stems represent less than 10 % d.w.of the overall above-ground grass silica content (e.g. Webb and Longstaffe, 2002), even in grasses with high stem biomass such as bamboos (e.g. (Ding et al., 2008). Stem phytoliths are weakly ^{18}O-enriched relatively to the soil water (Webb and Longstaffe, 2006). Thus, the contribution of stem phytoliths should slightly decrease $\delta'^{18}O_{Phyto}$ and increase $^{17}O\text{-excess}_{Phyto}$ average values. Assuming a $^{17}O\text{-excess}_{Phyto}$ difference between stem and bulk leaf of 200 per meg would lead to a $^{17}O\text{-excess}_{Phyto}$ value for stem (10 % d.w.) and leaf (90 % d.w.) phytolith assemblage higher by 20 per meg relatively to an only leaf phytolith assemblage, which is lower than the lowest reproducibility obtained when measuring 3 aliquots of phytoliths (23 per meg). Finally, neither grass height or grass anatomy should significantly impact the $^{17}O\text{-excess}_{Phyto}$.

Experiment 1 gives some tracks for assessing whether senescence may impact the $^{17}O\text{-excess}_{Phyto}$ vs RH relationship calibrated for grass leaf during elongation in Alexandre et al. (2018). In the case of *F. Arundinacea,* 58% of silica polymerization occurs at the transition between the end of the elongation stage and the beginning of the senescence stage, mainly in long cells and on cell walls. Leaf senescence is a stress-induced or age-related developmental aging during which transpiration decreases to minimal level but is still efficient (Norton et al., 2014), epidermal conductance progressively prevailing over stomatal conductance (Smith et al., 2006). If the cells already contain dissolved silica, epidermal evaporation, not balanced by water input due to decreasing transpiration, may lead to silica saturation and polymerization. Isotope fractionation due to evaporation during this process should follow the Craig and Gordon model. Thus, under similar climate conditions, the isotope compositions of leaf water and phytoliths formed when senescence occurs should not be different from the isotope composition of the bulk adult leaf blade that form during leaf elongation. This is in agreement with what is observed. However, in nature, senescence occurs due to seasonal climate change such as drastic decrease of RH in the tropical and Mediterranean areas. In these conditions, phytoliths formed during

senescence may have higher $\delta'^{18}O_{Phyto}$ and lower $^{17}O\text{-excess}_{Phyto}$ values than phytoliths formed during leaf elongation. Mere monitoring of stress-induced senescence effect on $^{17}O\text{-excess}_{Phyto}$ will determine whether RH prevailing at the beginning of senescence should be considered in addition to RH prevailing during leaf elongation when interpreting $^{17}O\text{-excess}_{Phyto}$.

Overall, the data and estimates presented here contribute to a more precise identification of the parameters to consider when using the $^{17}O\text{-excess}_{Phyto}$ *vs* RH relationship previously obtained (Alexandre et al., 2018). They additionally bring valuable elements to trace from phytoliths the triple oxygen isotope composition of grass leaf water, which influences the isotope signal of several processes at the soil/plant/atmosphere interface.

Technical corrections

Line 57: Do not use the term distillation processes. In one of the references you cite (Steig et al. 2014) a distillation experiment is conducted where 17Oexcess changes over 90per meg. Distillation processes can be governed both by equilibrium fractionation or kinetic fractionation depending on the set up.
This will be modified in the revised draft: The $\delta^{18}O$ and $\delta^{17}O$ combination varies weakly in precipitation (Angert et al., 2004; Barkan and Luz, 2007; Landais et al., 2008) and is not significantly affected by temperature (Barkan and Luz, 2005; Uemura et al., 2010), in contrast to the deuterium-excess (d-excess = $\delta^2H - 8.0 \times \delta^{18}O$).

Line 124: provide 1 significant digit for the d18O isotopic composition.
This will be corrected in the revised draft: -5.59 ‰ and 26 per meg for $\delta'^{18}O$ and ^{17}O-excess, respectively

Line 190: Please specify how the working O2 gas was calibrated relative to SMOW or point to Alexandre et al. 2018. Provide the SMOW calibrated values for the internal quartz laboratory standard (Boulangé) and explain how that calibration was done. Ideally, provide a comparison of this laboratory internal standard to international standards with published D17O on SMOW scale. This is crucial for recalculating the data in case of any revised calibration.

Phytoliths triple oxygen isotope analysis was performed as described in details in Alexandre et al. (2018). The IR Laser-Heating Fluorination Technique (Alexandre et al., 2006, Crespin et al., 2008; Suavet et al., 2010) was used to extract the O_2 gas after a dehydration and dehydroxylation under a flow of N_2 (Chapligin et al., 2010). The purified oxygen gas (O_2) was passed through a -114°CC slush to refreeze gases interfering with the mass33 (e.g. NF), potentially produced during the fluorination of residual N in the line, before being sent to the dual-inlet mass spectrometer (ThermoQuest Finnigan Delta Plus). The composition of the reference gas was determined through the analyses of NBS28 for which isotope composition has been set to $\delta^{18}O$ = 9.60 ‰ *vs* VSMOW, $\delta^{17}O$ = 4.99‰ *vs* VSMOW and ^{17}O-excess = 65 per meg. Each analysis consisted in two runs of eight dual inlet measurements with an integration time of 26s. The sample isotope compositions were corrected on a daily basis using a quartz laboratory standard (Boulangé) with $\delta^{18}O$ = 16.284 ‰ *vs* VSMOW, $\delta^{17}O$ = 8.463 ‰ *vs* VSMOW. During the measurement period, Boulangé reproducibility (SD) was ± 0.13 ‰, ± 0.07 ‰ and ± 11 per meg for $\delta^{18}O$, $\delta^{17}O$ and ^{17}O-excess respectively (n = 9). For a given sample from two to three phytoliths aliquots were analyzed. Measured reproducibility ranged from 5 to 23 per meg.

Line 215: Do you mean Figure 2 (not 1)?
Yes. This will be corrected in the revised draft.

Line 230: Table 1?
fig. 1, Table S2

Line 235:The good fit of the linear correlation seems impressive at first sight but the irrigation water is not included in that regression. If the linear regression (presented in the first manuscript version) is extrapolated, the irrigation water clearly falls below the line. I advise against using linear regressions because evaporation trends are best represented by curves.

Right. In the revised draft we will not refer to a regression line but simply mention that: In adult leaf waters, a clear evaporative fractionation trend occurs from the sheath to the proximal and apical blade. Water from the young leaf blade plots close to the adult apical blade.

Line 241: These _Phyto-LW are significantly lower than the expected equilibrium fractionation between silicates and water (_silica-water = 0.524 for the 5-35_C temperature range). The average reader won't remember that value so you may want to note that discrepancy here.
This will be corrected in the revised draft: $\lambda_{Phyto\text{-}LW}$ is lower than the 0.524 equilibrium $\lambda_{silica\text{-}water}$ value calculated from Sharp et al. (2016). It decreases from 0.522 in the sheath to 0. 521 and 0.520 in the proximal and apical parts of the blade, respectively (Table S2).

Line 252: Remind the reader that RH and T changed with the light/dark alternations in this experiment.
This will be corrected in the revised draft: In experiment 2b, where temperature and RH changed with light/dark alternations, transpiration and leaf blade phytolith concentrations do not change by more than 0.1L/day and 0.2% d.w., respectively, when light is set constant or alternates with dark (Table S1).

Line 287: The second ii) should be iii).
This will be corrected in the revised draft

Line 304: source not tsource.
This will be corrected in the revised draft

Table S3: If the leaf temperature is reduced from 20.4 to 18.4, the RH at the site of evaporation changes, so RH with respect to the leaf temperature (not air temperature) should be used as also recommended by Farquhar and Gan (2003).

In the revised draft, the leaf temperature will be kept and the discussion on atmospheric vs leaf temperature removed.

The Reference list is missing in the revised version.
The reference list will be added in the revised draft.

Caption of Fig. 3: 17_ = 18__ not 17_ = 17__
Clean up the legend of Fig. 3. (e.g. use _=0.52x)
Figure 3 and its caption will be modified (cf Figure 1 in the present answer).

References

Angert, A., Cappa, C.D., and DePaolo, D.J. (2004). Kinetic O-17 effects in the hydrologic cycle: Indirect evidence and implications. Geochim. Cosmochim. Acta *68*, 3487–3495.

Barkan, E., and Luz, B. (2005). High precision measurements of 17O/16O and 18O/16O ratios in H2O. Rapid Commun. Mass Spectrom. *19*, 3737–3742.

Barkan, E., and Luz, B. (2007). Diffusivity fractionations of H2(16)O/H2(17)O and H2(16)O/H2(18)O in air and their implications for isotope hydrology. Rapid Commun. Mass Spectrom. RCM *21*, 2999–3005.

Blunier, T., Barnett, B., Bender, M.L., and Hendricks, M.B. (2002). Biological oxygen productivity during the last 60,000 years from triple oxygen isotope measurements. Glob. Biogeochem. Cycles *16*, 3–1.

Cernusak, L.A., Barbour, M.M., Arndt, S.K., Cheesman, A.W., English, N.B., Feild, T.S., Helliker, B.R., Holloway-Phillips, M.M., Holtum, J.A.M., Kahmen, A., et al. (2016). Stable isotopes in leaf water of terrestrial plants. Plant Cell Environ. *39*, 1087–1102.

Ding, T.P., Tian, S.H., Sun, L., Wu, L.H., Zhou, J.X., and Chen, Z.Y. (2008). Silicon isotope fractionation between rice plants and nutrient solution and its significance to the study of the silicon cycle. Geochim. Cosmochim. Acta *72*, 5600–5615.

Farquhar, G.D., and Gan, K.S. (2003). On the progressive enrichment of the oxygen isotopic composition of water along a leaf. Plant Cell Environ. *26*, 801–819.

Helliker, B.R., and Ehleringer, J.R. (2000). Establishing a grassland signature in veins: 18O in the leaf water of C3 and C4 grasses. Proc. Natl. Acad. Sci. U. S. A. *97*, 7894–7898.

Kavanová, M., Lattanzi, F.A., Grimoldi, A.A., and Schnyder, H. (2006). Phosphorus Deficiency Decreases Cell Division and Elongation in Grass Leaves. Plant Physiol. *141*, 766–775.

Kumar, S., and Elbaum, R. (2017). Interplay between silica deposition and viability during the life span of sorghum silica cells. New Phytol.

Kumar, S., Milstein, Y., Brami, Y., Elbaum, M., and Elbaum, R. (2016). Mechanism of silica deposition in sorghum silica cells. New Phytol. *213*, 791–798.

Kumar, S., Adiram-Filiba, N., Blum, S., Sanchez-Lopez, J.A., Tzfadia, O., Omid, A., Volpin, H., Heifetz, Y., Goobes, G., and Elbaum, R. (2019). Grass silica mineralizer (GSM1) protein precipitates silica in sorghum silica cells. BioRxiv 518332.

Landais, A., Barkan, E., and Luz, B. (2008). Record of δ18O and 17O-excess in ice from Vostok Antarctica during the last 150,000 years. Geophys. Res. Lett. *35*, L02709.

Norton, M.R., Lelièvre, F., and Volaire, F. (2014). Measuring dehydration tolerance in pasture grasses to improve drought survival. Crop Pasture Sci. *65*, 828–840.

Sharp, Z.D., Gibbons, J.A., Maltsev, O., Atudorei, V., Pack, A., Sengupta, S., Shock, E.L., and Knauth, L.P. (2016). A calibration of the triple oxygen isotope fractionation in the SiO2–H2O system and applications to natural samples. Geochim. Cosmochim. Acta *186*, 105–119.

Skinner, R.H. (usda, and Nelson, C.J. (1995). Elongation of the grass leaf and its relationship to the phyllochron. Crop Sci. USA.

Smith, S.E., Fendenheim, D.M., and Halbrook, K. (2006). Epidermal conductance as a component of dehydration avoidance in Digitaria californica and Eragrostis lehmanniana, two perennial desert grasses. J. Arid Environ. *64*, 238–250.

Steig, E.J., Gkinis, V., Schauer, A.J., Schoenemann, S.W., Samek, K., Hoffnagle, J., Dennis, K.J., and Tan, S.M. (2014). Calibrated high-precision 17O-excess measurements using cavity ring-down spectroscopy with laser-current-tuned cavity resonance. Atmospheric Meas. Tech. *7*, 2421–2435.

Surma, J., Assonov, S., Herwartz, D., Voigt, C., and Staubwasser, M. (2018). The evolution of 17 O-excess in surface water of the arid environment during recharge and evaporation. Sci. Rep. *8*, 4972.

Uemura, R., Barkan, E., Abe, O., and Luz, B. (2010). Triple isotope composition of oxygen in atmospheric water vapor. Geophys. Res. Lett. *37*, L04402.

Webb, E.A., and Longstaffe, F.J. (2006). Identifying the δ 18O signature of precipitation in grass cellulose and phytoliths: Refining the paleoclimate model. Geochim. Cosmochim. Acta *70*, 2417–2426.

Supplementary material (cf excel file)

Table S1. Growth chamber experiment 2a and 2b. Experimental set-up, phytolith content and triple oxygen isotope data obtained for phytoliths (Phyto), leaf water (LW) and irrigation water (IW). Samples are named according to the climate chamber # they were collected in (e.g. F4), the date of sampling (dd/mm/yy) and the sampling after day or night (Day vs Night in experiment 2a) or after constant climate conditions or day/night alternation (Cst vs DN in experiment 2b). n : number of replicates ; SD : standard deviation calculated on the replicates; Phyto Conc. (% d.w.) stands for phytolith concentration expressed in % of the dry weight.

Table S2. Growth chamber experiment 1 : Experimental set-up, phytolith content, phytolith morphological assemblages and triple oxygen isotope raw data obtained for phytoliths (Phyto), leaf water (LW), irrigation (IW) and phytolith-forming water (FW). n : number of replicates ; SD : standard deviation calculated on the replicates; Phyto Conc. (% d.w.) stands for phytolith concentration expressed in % of the dry weight. "Adult leaves: bulk blade av." stands for the weighted average of values obtained for proximal and apical blade samples. "% d.w." stands for % dry weight. Phytolith proportion in senescent leaves was calculated using a mass loss correction factor of 0.7 for (see text for explanation).

Table S3. $\delta^{18}O$, $\delta^{17}O$ and ^{17}O-excess predicted for bulk leaf water (LW) and phytolith (Phyto) according to the Craig and Gordon model adapted to leaf water by Farquhar et al. (2007). After spreadsheet provided in Cernusak et al. (2016). For the water-vapor couple, the equilibrium and kinetic fractionation $^{17}\alpha_{eq}$ and $^{17}\alpha_K$ are calculated using $^{17}\alpha_{eq}={}^{18}\alpha_{eq}{}^{0.529}$ and $^{17}\alpha_k={}^{18}\alpha_k{}^{0.518}$. Source water is set equivalent to irrigation water (IW). For the silica-water couple, the fractionation factor $^{17}\alpha$ is calculated following $^{17}\alpha = {}^{18}\alpha^{\lambda_{silica\text{-}water}}$ with $\lambda_{silica\text{-}water}$ set at 0.522 and 0.521. A mixing hypothesis is added to the Craig and Gordon model, assuming a mixing between irrigation water and evaporated water estimated from the Farquhar and Gan (2003) model.

Table S4. $\delta^{18}O$, $\delta^{17}O$ and ^{17}O-excess predicted for 1) leaf water (LW) along the blade according to the Farquhar and Gan (2003) equations 2, 3 and 5 and assuming a radial Péclet number of zero and **2) phytoliths (Phyto) along the blade using $^{18}\alpha_{silica\text{-}water}$ from Dodd and Sharp (2010), and $\lambda_{silica\text{-}water}$ equivalent to 0.524 (Sharp et al., 2016), 0.522 and decreasing from 0.522 to 0.520 from base to apex.** See Farquhar and Gan (2003) for definition of the parameters. For the water-vapor couple, the equilibrium and kinetic fractionation $^{17}\alpha_{eq}$ and $^{17}\alpha_K$ are calculated using $^{17}\alpha_{eq}={}^{18}\alpha_{eq}{}^{0.529}$ and $^{17}\alpha_k={}^{18}\alpha_k{}^{0.518}$. Source water is set equivalent to irrigation water (IW). For the silica-water couple, the fractionation factor $^{17}\alpha$ is calculated following $^{17}\alpha = {}^{18}\alpha^{\lambda silica\text{-}water}$.